The line-driven instability

Achim Feldmeier

University of Kentucky, Lexington, KY 40503, USA (achim@pa.uky.edu)

Abstract. The line-driven instability may cause pronounced structure in winds of hot, luminous stars, e.g., fragments of dense shells, strong reverse shocks, and fast cloudlets. We discuss the linear stability theory, including the line-drag effect, phase reversal due to the diffuse radiation field, and the relevance of so-called Abbott waves. Recent hydrodynamic simulations focuss on the influence of a time-dependent source function on the flow structure, and on the X-ray emission from wind shocks and cloud collisions.

1 Introduction

Lucy & Solomon (1970) described a new, *line-driven* instability for OB star winds, which may be connected to (some of) the following observational facts: (i) the appearence of discrete absorption components, periodic absorption modulations, black troughs, and variable blue edges in P Cygni line profiles (see reviews by Fullerton, Henrichs, Kaper, Kaufer, or Massa in this volume); (ii) the X-ray emission from hot star winds, and their superionization; and (iii) cloud formation in O star and Wolf-Rayet star winds (Moffat 1994).

In the following we shall discuss some aspects of the instability from a mostly hydrodynamical viewpoint.

2 Linear theory

2.1 Mechanism of the instability

MacGregor et al. (1979) and Carlberg (1980) calculated growth rates for the line-driven instability assuming optically thin flow perturbations. Contrary, Abbott (1980) found zero growth rates when he applied the Sobolev approximation to the perturbations. He found then a new type of marginally stable, radiative-acoustic waves, which we shall term 'Abbott waves' in the following. Owocki & Rybicki (1984) unified these contradictory results by showing that they refer to different wavelength regimes λ of the perturbations, namely $\lambda < L$ (with L being the Sobolev length) in the work of MacGregor et al. and Carlberg, while $\lambda \to \infty$ in Abbott's analysis.

The regime $\lambda > L$ or $\lambda \gg L$ in between these extremes is especially interesting: while the growth rate drops there as $\Omega \propto \lambda^{-2}$, the instability is very strong ($\Omega_{\max}\ t_{\rm flow} \approx 50$; Owocki & Rybicki 1984), so that even rather

long-scale perturbations can grow into saturation, and become the most pronounced flow structures in terms of velocity, density, and temperature jumps. Having wavelengths larger than the Sobolev length, these perturbations can be viewed as *unstable* Abbott waves: the propagation speed follows from the usual, first order Sobolev treatment, whereas the small growth rate is of second order (Feldmeier 1998).

The physical basis of the instability for different wavelength regimes is illustrated in Fig. 1: region (a) shows an unstable short-scale perturbation, $\lambda = \mathrm{O}(L)$ (where L corresponds to the 'thickness' of the thermal band, indicated in the plot by double lines): an arbitrary, positive velocity fluctuation shifts the gas parcel out of the absorption shadow of gas lying closer to the star, and the enhanced flux accelerates the parcel to even larger speeds, deshadowing it further. With the line force scaling as $g_l \propto \exp(-\tau)$, the general instability cycle can be written $\delta v \rightarrow -\delta\tau \rightarrow \delta g_l \rightarrow \delta v$. Region (b) around the node of a long-scale, sinusoidal perturbation shows the occurence of inward propagating Abbott waves from first order Sobolev approximation: the steepening of the thermal band at the node raises the Sobolev line force, $g_l \propto v'^{\alpha}$ (where $v' = dv/dr$, and $0 < \alpha < 1$), and the gas is accelerated to larger speeds. This corresponds to an inward shift of the node, i.e., an inward phase propagation of a wave. The wave cycle can be written $\delta v' \rightarrow \delta g_l \rightarrow i\delta v \rightarrow -\delta v'$. Finally, region (c) around the velocity maximum of the long-scale perturbation shows that this Abbott wave is unstable from a second order treatment: due to the negative curvature of the thermal band the optical depth is *smaller* there than for the unperturbed flow. Again, a larger line force results which accelerates the gas; this now makes the maximum more pronounced, wherefore $-v''$ increases *further* (we assumed here that the node separation or wavelength is essentially unaffected). Thereby, τ drops further, g_l grows further, and one has unstable growth. The general instability cycle can then be further specified to become $-\delta v'' \rightarrow -\delta\tau \rightarrow \delta g_l \rightarrow \delta v \rightarrow -\delta v''$. Notice also the kinematical steepening and finally braking of the wave into a strong reverse shock.

2.2 Information propagation

Yet, this unified picture of Abbott waves and the line-driven instability is oversimplified. In a remarkable paper, Owocki & Rybicki (1986) show from a Green's function analysis that *information propagation* in an unstable, pure *absorption* line flow is limited to the sound speed; contrary, radiative-acoustic waves propagate inward at a phase or group speed equal to the much larger (negative) wind speed (Abbott 1980).

This is an example of the non-equivalence of signal or information speed and group speed in unstable media (e.g., Bers 1983).

To demonstrate this physically, Owocki & Rybicki (1986) consider a Gaussian pulse which is broader than the Sobolev length, and therefore should propagate upstream at the wind (or Abbott) speed. This is indeed confirmed,

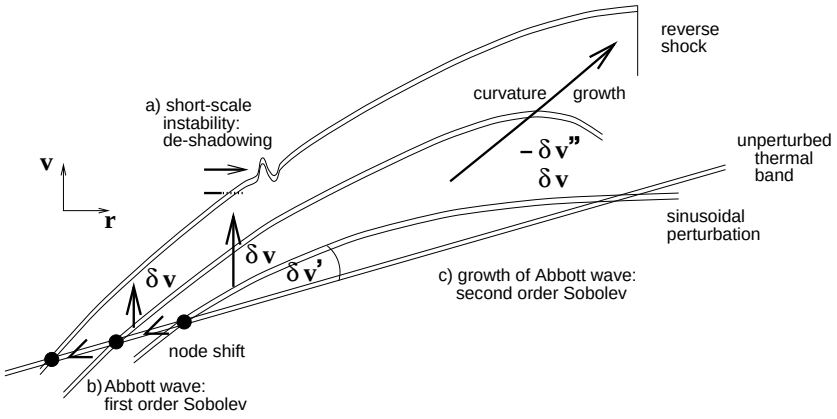

Fig. 1. Line-driven instability and Abbott waves.

even when the Green's function for zero sound or signal speed is used to propagate the pulse! However, Owocki & Rybicki (1986) claim that no *signal* is propagated in this case. Namely, due to its smoothness, information is not localized in the pulse, and properties from any small neigborhood can be used to infer distant properties via a Taylor series expansion, without need for information propagation.

That this is the case in the above example (i.e., that the folding of the Green's function with the signal is equivalent to a Taylor series extrapolation of a smaller to a larger space-time area) is seen if a truly localized information is introduced into the pulse, here by setting its amplitude to zero for all $x > x_0$, with arbitrary x_0. In accord with $a = 0$, the discontinuity at x_0 does not propagate, but remains there. For $x < x_0$ then, the *full*, smooth Gaussian *without* any discontinuity is reconstructed in course of time, and propagates upstream to smaller x! This awkward fact is due to the one-sidedness of the pure absorption line force, i.e., that a perturbation at $x > x_0$ cannot affect the upstream flow at $x < x_0$. Since for $x < x_0$ all derivatives, curvatures, etc. are those of the *full* Gaussian, the latter is reconstructed for $x < x_0$, and propagates upstream as a 'false' signal. We leave here out a discussion of the region $x > x_0$.

The key point in this discussion is the one-sidedness of the absorption line force, and the situation could be fundamentally different for a non-zero source function. Corresponding numerical simulations show then indeed the inward propagation of a front at Abbott speed following a delta-function perturbation (Owocki & Puls 1998).

One reason it is important to decide whether Abbott waves are real are recent claims on the role of *kinks* in the wind velocity law, which propagate upstream at Abbott speed (for corotating intercation regions: Cranmer &

Owocki 1996; for wind clouds: Feldmeier et al. 1997b). Future analytical work will hopefully bring further clarification.

2.3 The line-drag effect

Besides for these matters of wave propagation, which we shall take up again in the next section, line scattering is also important for instability growth rates. Lucy (1984) questioned the occurence of the line-driven instability in hot star winds altogether, by noting that the winds are driven essentially by scattering lines (as opposed to absorption lines), and that the *diffuse* radiation field should cancel any extra line force gained by Doppler-shifting gas into the *direct* radiation field.

However, this exact cancellation occurs only near the star, at the wind base. Due to sphericity effects and the decreasing angular size of the stellar disk with distance, the growth rate is back to 50% of its pure absorption line value within a stellar radius of the stellar surface, and approaches 80% of this value at large radii (Owocki & Rybicki 1985).

The line-drag is therefore most relevant in deep wind layers, and may be important with regard to the photosphere-wind connection, i.e., whether the formation of wind structure is externally triggered or self-excited.

3 Numerical simulations

3.1 SSF and EISF

While line scattering is of central importance for the formation of wind structure, the exact solution to the radiative transfer equation in instability simulations is prohibitively cpu-time consuming. The 'smooth source function' approximation (SSF; Owocki 1991) uses instead a formal integral approach, assuming a prespecified source function from Sobolev approximation. Via this averaged or mean diffuse radiation field, the line-drag effect is incorporated in SSF calculations.

One-dimensional numerical simulations for a spherically symmetric O star wind (Owocki et al. 1988; Owocki 1992) perturbed by a harmonic, photospheric sound wave show that the continuous flow breaks up into a sequence of strong reverse shocks, each decelerating inner, thin, fast gas and compressing it into narrow, dense shells. The shells propagate roughly according to a stationary wind velocity law. For a discussion of self-excited wind structure and issues of periodic vs. chaotic wind structure, we refer to Owocki (1994).

Recently, Owocki & Puls (1996, 1998) proposed a new, 'escape integral source function' approximation (EISF) which accounts for the first time for the *perturbed* diffuse radiation field. The idea is here to replace the photon escape probabilities, β_s, from the smooth, Sobolev source function, $S = \langle \beta_s I_* \rangle / \langle \beta_s \rangle$ (brackets indicate angle averaging) at each time step with the

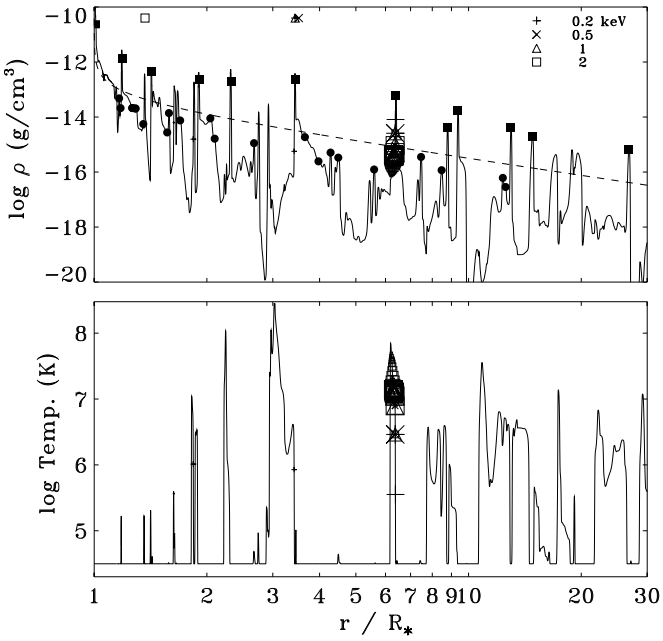

Fig. 2. Density and temperature snapshot for a wind model of ζ Ori. Filled bullets mark fast cloudlets, filled squares mark dense shells. Symbols (+, ×, etc.) indicate strong X-ray emission at the given energies.

escape probabilities from the time-dependent wind simulation, β_i. The β_i are the central quantities which distinguish instability simulations from stationary wind models applying the Sobolev approximation, since they include both (de-)shadowing effects of neighboring and widely separated gas parcels.

As Puls et al. (1994) noticed, the inclusion of the correct diffuse radiation field is important since, as was shown by Owocki & Rybicki (1985) from an exact, linear analysis, the perturbed diffuse radiation field can turn anti-correlated, inward propagating density and velocity fluctuations into correlated, outward propagating fluctuations. In the nonlinear, wave braking phase, the former steepen into reverse shocks, the latter into forward shocks. SSF calculations show the dominance of reverse shocks. The question is whether EISF simulations are instead dominated by forward shocks.

The answer is essentially 'no'. A phase reversal occurs only for short-scale fluctuations below the Sobolev length (Owocki & Rybicki 1985). Steepening the thermal band over short lengthscales until it becomes optically thin – and hence the instability ceases since no further de-shadowing is possible – leads

only to small velocity jumps of order the thermal speed. The EISF structure appears therefore as short-scale, low-amplitude noise superimposed on the long-scale, large-amplitude sequence of reverse shocks. Still, these results indicate that the Sobolev length as an intrinsic lengthscale of line-driven flows separates two different regimes of the (inverse) turbulent cascade. Caution is therefore required in applying results from, e.g., supersonic Burgers turbulence to hot star winds. Furthermore, we add here that cloudlets which are important for the X-ray emission from O stars (cf. the next section) have lengthscales not too different from the EISF noise. Since the cloudlets are anti-correlated perturbations, future simulations have to show whether they are affected by the inclusion of the perturbed diffuse radiation field. Finally, we refer to Owocki & Puls (1998) for a discussion of the modifications of the *stationary* solution for thin winds due to the inclusion of fore-aft asymmetric (e.g.: EISF) escape probabilities around the sonic point, which are not present in usual Sobolev approximation.

3.2 X-ray emission

One main interest in the line-driven instability is that it may create shocks which are responsible for the observed X-ray emission from hot star winds, and partially (Pauldrach 1987) also for their superionization.

After overcoming numerical problems which lead to a collapse of cooling zones (Cooper & Owocki 1992; Feldmeier 1995), the temperature structure behind strong reverse shocks can be calculated (Fig. 2), and their X-ray emission synthesized. For the self-absorption of X-rays in the dense wind shells, NLTE opacities from stationary wind models are presently used (Feldmeier et al. 1997a).

In agreement with estimates by Hillier et al. (1993) from properties of reverse shocks as deduced from isothermal wind simulations, we find that these shocks can only account for 1 to 10% of the observed X-ray emission during their quasi-steady appearance, i.e., when thin, fast gas is being fed through the front. However, by applying chaotic perturbations at the wind base, we find that short, strong X-ray flashes in the wind can account for the observed X-ray emission, even after time-averaging. The flashes originate from collisions of small, fast cloudlets with the pronounced, dense wind shells (Feldmeier et al. 1997a). Both the continuous stream of thin gas and the discrete cloudlets are ablated from gas which moves ahead (i.e., at somewhat larger radii) of the next inner, pronounced shell. The shells and cloudlets are indicated in Fig. 2.

So far the modeling assumes a spherically symmetric, radial wind (for first 2-D instability simulations, see Owocki, this volume), and leads to major variability in X-ray fluxes. However, cloudlets which form due to photospheric turbulence should have a rather small lateral scale. With independent cloud-shell collisions taking place along neighboring wind cones, (near) constancy of X-ray fluxes should then be achieved by angle averaging (Cassinelli & Swank

1983). The present, 1-D wind models suggest that a few thousand wind cones should be sufficient to achieve the observed flux constancy.

On the other hand, the pronounced shells possibly form due to long-periodic, coherent photospheric perturbations, wherefore their lateral scale may be large, and they may extend over many such neighboring wind cones. Possibly, larger shell segments fragmentize due to the Rayleigh-Taylor instability. Future 2-D simulations have to bring clarification.

Acknowledgements. I thank J. Cassinelli, A. Fullerton, R.P. Kudritzki, C. Norman, S. Owocki, A. Pauldrach, J. Puls, and I. Shlosman for many interesting discussions. I thank the organizers of this meeting for a generous travel grant. Work in this project was funded by DFG projects Pa 477/1-1 and 1-2, and by NASA grant NAG 5-3841.

References

Abbott D.C., 1980, ApJ 242, 1183
Bers A., 1983, in Galeev A.A., Sudan R.N. (eds.) Handbook of Plasma Physics, Vol. 1. North Holland, Amsterdam, 451
Carlberg R.G., 1980, ApJ 241, 1131
Cassinelli J.P., Swank J.H., 1983, ApJ 271, 681
Cooper R.G., Owocki S.P., 1992, PASPC 22, 281
Cranmer S.R., Owocki S.P., 1996, ApJ 462, 469
Feldmeier A., 1995, A&A 299, 523
Feldmeier A., 1998, A&A 332, 245
Feldmeier A., Puls J., Pauldrach A.W., 1997a, A&A 322, 878
Feldmeier A., Norman C., Pauldrach A.W., et al., 1997b, PASPC 128, 258
Hillier D.J., Kudritzki R.P., Pauldrach A.W., et al., 1993, A&A 276, 117
Lucy L.B., 1984, ApJ 284, 351
Lucy L.B., Solomon P.M., 1970, ApJ 159, 879
MacGregor K.B., Hartmann L., Raymond J.C., 1979, ApJ 231, 514
Moffat A.F., 1994, Rev. Mod. Astron. 7, 51
Owocki S.P., 1991, in Crivellari L., et al. (eds.) Stellar atmospheres: beyond classical models. Kluwer, Dordrecht, 235
Owocki S.P., 1992, in Heber U., Jeffery S. (eds.) The atmospheres of early-type stars. Springer, Heidelberg, 393
Owocki S.P., 1994, Ap&SS 221, 3
Owocki S.P., Puls J., 1996, ApJ 462, 894
Owocki S.P., Puls J., 1998, ApJ, in press
Owocki S.P., Rybicki G.B., 1984, ApJ 284, 337
Owocki S.P., Rybicki G.B., 1985, ApJ 299, 265
Owocki S.P., Rybicki G.B., 1986, ApJ 309, 127
Owocki S.P., Castor J.I., Rybicki G.B., 1988, ApJ 335, 914
Pauldrach A.W., 1987, A&A 183, 295
Puls J., Feldmeier A., Springmann U., Owocki S.P., Fullerton A.W., 1994, Ap&SS 221, 409